Odor Assessment of Automobile Cabin Air by Machine Olfaction

J. Li, R. D. Hodges, S. S. Schiffman, H. T. Nagle
Department of Electrical and Computer Engineering
North Carolina State University
Raleigh, NC, USA

R. Gutierrez-Osuna
Department of Computer Science and Engineering
Texas A&M University
College Station, TX, USA

G. Luckey, J. Crowell
Materials Development Department
Hyundai Motor Group
Superior Township, MI, USA

***Abstract*—Odor quality in the cabin air of automobiles can be a significant factor in the decision to purchase a vehicle and the overall customer satisfaction with the vehicle over time. Current standard practice uses a human panel to rate the vehicle cabin odors on intensity, irritation, and pleasantness. However, human panels are expensive, time-consuming and complicated to administer. To address this issue, we have developed a machine olfaction approach to assess odors inside automobiles for the purpose of enhancing or replacing the human panel by evaluating the correlation between the system performance and a trained human panel. Our approach employs an ion-mobility spectrometer and a photoionization detector for measuring volatile organic compounds inside automobiles. Our olfactory system achieves good correlations (range from 0.72 to 0.84) with a trained human panel using predictive models generated by linear regression and cross-validation. Our results support the feasibility of replacing human panel assessments by a machine olfaction system.**

Keywords—machine olfaction; ion mobility spectrometry; photoionization; air quality; odor assessment; volatile organic compounds; principal components analysis; linear regression

I. Introduction

Odors inside vehicles, especially new vehicles, arise from volatile organic compounds (VOCs) emitted from interior materials, including leather, plastic, carpet, vinyls, paint and glues. The odor quality can affect customers' satisfaction and their health over time. In a key study [1], GC/MS measurements indicated a large number of undesirable VOCs inside tested automobile cabins, including many aliphatic hydrocarbons and aromatic hydrocarbons. Although odors are determined by their chemical constituents, chemical analytical techniques are unable to detect the interaction between different chemicals and to evaluate the resulting odor quality. For this reason, trained human panels have been used traditionally to evaluate the air quality inside automobiles [2]. However, human panels introduce important constraints. Their time is very valuable; they can suffer respiratory inflammation; they experience age-related sensory alterations; and their ratings can be adversely impacted by medications. Also, a complete and detailed odor linguistic description and sophisticated panel training are key factors in generating accurate odor measurements. Furthermore, instrumental methods are needed to reduce the human panel exposure to undesirable chemical compounds during odor evaluation tests and improve costefficiency. Therefore, machine olfaction is proposed to substitute for (or to assist) humans in odor assessment roles.

Over the past 30 years, machine olfaction devices have been utilized to detect and identify odorants in a wide variety of commercial industries such as agricultural [3], food manufacturing [3-6], fragrance and cosmetics production [7], environmental monitoring [3], pharmaceuticals [3, 8, 9], and medical diagnosis [3, 10, 11]. These systems consist of an array of odor sensors to generate patterns of response and signal processing algorithms to recognize and analyze the patterns.

In this project, we employed two chemical detection instruments (a Lonestar ion mobility spectrometer (IMS) by Owlstone, Inc., and a ppbRAE PGM-7240 photoionization detector by RAE Systems, Inc.), combined with signal processing methods, to implement our machine olfaction system. This paper is organized as follows. In Section II we present and discuss a methodology along with the experimental setup. The system block diagram is also described in this section. The results of experiments are presented and discussed in Section III. Our conclusions and future work are presented in Section IV.

II. Experiments and Methodologies

A. System design

The odor evaluation by the human panel is described in Fig. 1. The odor sample is presented to four trained panel members who each give their ratings using three scales within a range from 0 to 8: intensity, irritation, and pleasantness [12]. Scale 0 means no odor intensity, no irritation intensity and extremely pleasant, respectively. Scale 8 means maximal odor intensity, maximal irritation intensity and extremely unpleasant, respectively. Pleasantness scale rating 4 is neutral.

The machine olfaction system we designed aims to achieve the same function as the human panel, and to efficiently provide repeatable measurements over extended periods of time. The components of the system are shown in Fig. 2.

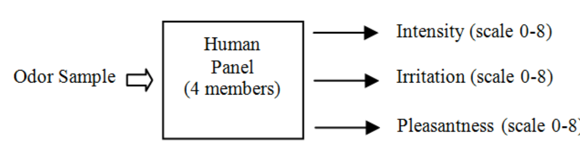

Fig. 1. Human-panel odor rating method [12].

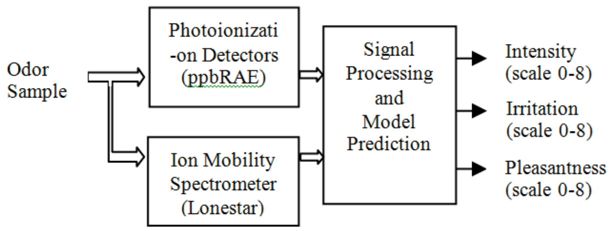

Fig. 2. Machine-based assessment approach.

When the same odor sample is presented to both the human panel in Fig.1 and the machine olfaction system in Fig. 2, both should generate similar ratings for odor intensity, irritation and pleasantness. Therefore with appropriate training and periodic maintenance, the designed machine olfaction system should be able to replace human panels to evaluate the odor quality in environments that are unhealthy or stressful to human subjects, such as inside heat-cycled automobile cabins.

Ten different vehicles were selected from five car models. Each model had two vehicles (one interior with cloth and the other with leather). Each vehicle was odor-tested before and after the heating cycle. Heating an automobile in a test chamber can simulate situations during sun exposure in warm climates. Therefore, in our total dataset consisted of 20 odor samples; each vehicle had one pre-heated (cold) sample and a second post-heated (hot) sample.

Each sample was assessed by the human panel, the ppbRAE and the Lonestar in rapid succession. First, the sample air from vehicle cabin was directed to the Lonestar instrument by Tygon® tubing connected through the test chamber as shown in Fig. 3. The Lonestar ionized each sample and generated a positive dispersion field (DF) matrix and a negative DF matrix for each measurement. Both matrices have a dimension 51×512 (see Fig. 4).

The Lonestar IMS uses a radiation source to ionize the molecules in the air stream. This airstream transverses a conductive channel in which an alternating asymmetric electric field is applied along with a DC bias, which is swept as the amplitude of the alternating field is increased. Ions that reach the end of the channel (those that avoid colliding with the walls) are detected producing a current proportional to the number of ions surviving the channel's electric field dynamics. A dispersion field matrix is the measured ion current as a function of applied DC bias and the amplitude of the applied asymmetric alternating electric field. This leads to a unique signature (image) for ions with the same mobility.

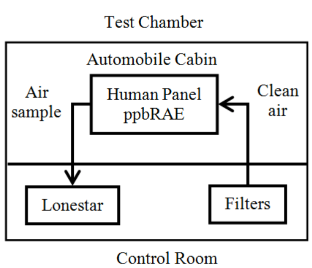

Fig. 3. Experiments diagram.

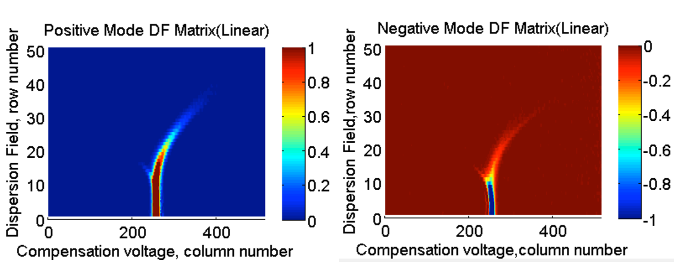

Fig. 4. Example postive and negative DF matrices.

Then, the four members of human panel entered the vehicle cabin wearing filtered masks. At the designated time, they took off mask and sniffed the odor. After sniffing, they rated the odor using the nine-level scales for intensity, irritation and pleasantness. Those scales were assigned based on reference odor samples that they encountered during training. One panelist also operated the ppbRAE inside each automobile to measure the peak and average concentration of total volatile organic compounds over a measurement period.

B. *Signal processing methods*

The flow chart of our signal processing module is shown in Fig. 5. Preprocessing and dimensionality reduction are included to extract the odor information from sensor data. A prediction model derived from linear regression can give estimated odor ratings. The performance of the prediction model is verified by the human panel measurements via cross-validation. The basic principles and employed methods are presented below.

1) Preprocessing

A number of preprocessing methods, including drift compensation, root mean squares (RMS), Gaussian and gradient filters, and normalization, were explored to compensate the acquired measurements [13]. Baseline manipulation can enhance contrast and compensate signal drift. Our data were collected in two one-week periods, separated by about 60 days. Drift compensation by independently removing the average bias of each one-week dataset gave the best performance. Next we performed normalization to improve subsequent feature extraction and pattern recognition by transforming the data to lie on a hyper-sphere of unit radius (removing the effect of units). This also transforms all the measurements to comparable magnitudes for numerical accuracy.

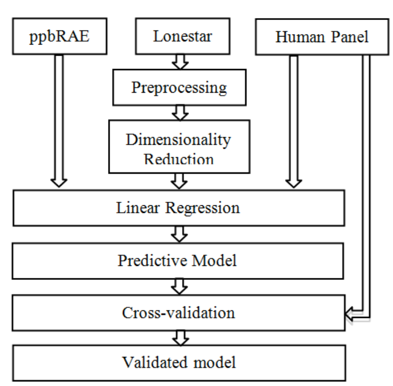

Fig. 5. Signal processing flow chart.

2) Dimensionality reduction

Since the Lonestar measurements have large dimensions (two matrices of dimension 51×512 for each sample), dimensionality reduction is essential to reduce the computational load and to extract data features without redundancy and collinearity. Principal components analysis (PCA) is the most commonly used dimension reduction method in machine olfaction applications. This method generates projections along the directions of maximum variance C (dimensions $n \times n$) of the sample data matrix X (dimensions $m \times n$). The number of samples is $m = 20$, and $n = 2 \times 51 \times 512 = 52224$ is the measurement's dimension. Since columns of X in our application represent the properties, and rows of X represent different samples, the covariance of X is a square matrix with large dimension 52224×52224 and traditional mathematical manipulations are computationally intensive. Thus, a "snapshot" PCA approach [13] was used instead of the traditional method. The advantage of this "snapshot" technique is that the covariance matrix is calculated based on the samples instead of properties, which saves a large amount of computing resources. The algorithm of the "snapshot" PCA method is shown below [14].

$$R = (X - \mu) \cdot (X - \mu)^T, \qquad Ra_j = \lambda_j a_j, \qquad j = 1, \cdots, m$$

$$e_j = \sum_{k=1}^{m} a_{k,j} X_k, \qquad \bar{e}_j = e_j \Big/ \sqrt{\sum_{i=1}^{n} (e_{j,i})^2}$$

$$V = [\ \bar{e}_1; \ \ \bar{e}_2; \ \ \cdots \ \ \bar{e}_m \ ], \qquad Y = X \cdot V^T$$

$$a_j = \begin{bmatrix} a_{1,j} \\ \vdots \\ a_{m,j} \end{bmatrix}, \qquad X_k = \begin{bmatrix} X_{k,1} \\ \vdots \\ X_{k,n} \end{bmatrix}^T, \qquad e_j = \begin{bmatrix} e_{j,1} \\ \vdots \\ e_{j,n} \end{bmatrix}^T$$

where μ is the column mean of X and expanded to the dimensions of X. $a_{i,j}$ is the constant coefficient for each sample. R is the sample inner product matrix and defined for calculating $a_{i,j}$. e_j is the j^{th} eigenvector and λ_j is the j^{th} eigenvalue of X. $\bar{e}_j$ is the normalized eigenvector e_j. V is generated by ordering the normalized eigenvectors from largest ($\bar{e}_1$) to smallest retained ($\bar{e}_m$). Y *is* the principal components matrix.

3) Linear regression

We used two linear regression techniques to build a predictive model for the relationship between odor quality measures (intensity, irritation, and pleasantness) and sensor responses: principal components regression (PCR) [15] and partial least squares (PLS) [16]. PCR uses the principal components of the data as regression variables. PCR can avoid collinearity problems, but its accuracy may be affected since it is an unsupervised method. In contrast, PLS extracts "latent variables" from the directions of maximum correlation between dependent and independent variable matrices in a sequential fashion. Each latent variable is generated iteratively, and the stopping point is determined by cross-validation.

4) Cross-validation

The accuracy of the predictive model was examined via K-fold cross-validation, where $N(K-1)/K$ samples were used for training, and N/K samples for testing. In order to avoid sample bias, samples from the same vehicle were kept in the same set (i.e. training or test) during the partitioning process, so a leave-one-vehicle-out procedure was adopted. Our sample size was limited to 20, setting our maximum K at 10.

III. Results and Discussion

First the Lonestar data was processed by the "snapshot" PCA method. Fig. 6 is the cumulative variance according to the 20 generated eigenvalues, indicating that only 8 principal components (PCs) are needed to capture 99% of the variance. Hence, we drop the other 12 PCs from further consideration.

The similarity between the Lonestar data and the human panel data were evaluated by correlation coefficients between the first 8 PCs and the three parameters of the human panel assessments (intensity, irritation and pleasantness). The results in Table 1 indicate that the second PC has the largest correlation with the human panel data.

We expected the correlation to be highest for the first PC, so we devised a method to address this issue. Since our data was collected during two different time periods, we divided the data into two subsets and removed the baseline of each separately, and then merged them back into a single dataset. This made the best correlation switch from the Lonestar's second PC to the first as shown in Table 2. Since the first PC has the highest weight in Fig. 6, this means that the similarity between the Lonestar measurements and the human panel's data has been enhanced by our drift compensation operation. To reduce computational complexity, at this point we decided to focus further processing on the first three PCs because they had high correlation with the human panel ratings and capture about 98% of the variance (see Fig. 6).

Three versions of the PCR regression model were generated using three different sets of independent variables: (1) the first three PCs (PC 1, 2, 3); (2) the two highest correlated PCs (PC 1, 2); and (3) the highest correlated PC (PC 1). Correlation coefficients between the PCR model's predicted and the original human panel evaluations are summarized in Table 3. The model with PC 1, 2 as independent variables has the highest correlation.

Next we performed PLS regression modeling. The correlation between PLS predictions and the human panel ratings is better than that calculated with PCR (see Table 3).

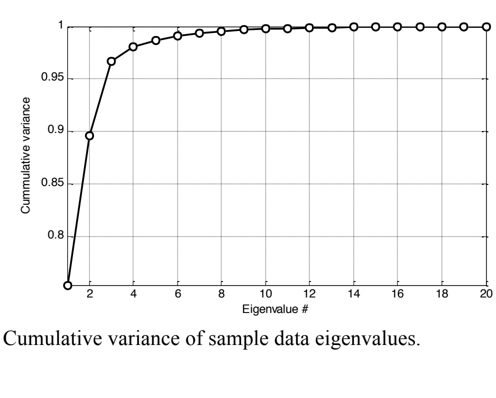

Fig. 6. Cumulative variance of sample data eigenvalues.

The independent ppbRAE total VOC measurements were analyzed and also show good correlation with the human panel's ratings (intensity 0.709, irritation 0.665 and pleasantness 0.752). We combined both the Lonestar and ppbRAE datasets to build additional regression models with improved prediction accuracy. Both PCR and PLS methods were employed with the combined datasets. The results are also shown in Table 3 (the last two rows). The combined feature vector generated more accurate predictions than either instrument alone. Table 3 illustrates that the PLS method has better performance than the PCR in this case.

TABLE I. CORRELATION BETWEEN LONESTAR MEASUREMENTS AND HUMAN PANEL DATA

Principal Components	Intensity	Irritation	Pleasantness
1	-0.297	-0.296	-0.305
2	**-0.688**	**-0.575**	**-0.709**
3	-0.470	-0.411	-0.489
4	-0.252	-0.061	-0.270
5	0.047	0.290	0.002
6	0.027	0.009	0.113
7	-0.169	-0.166	-0.098
8	-0.081	-0.317	-0.184

TABLE II. CORRELATION BETWEEN LONESTAR MEASUREMENTS AND HUMAN PANEL DATA AFTER PREPROCESSING

Principal Components	Intensity	Irritation	Pleasantness
1	**0.721**	**0.634**	**0.747**
2	-0.390	-0.403	-0.410
3	-0.398	-0.235	-0.459
4	-0.129	0.133	-0.142
5	0.100	0.095	0.175
6	0.219	0.247	0.158
7	0.202	0.328	0.169
8	0.002	-0.150	0.022

TABLE III. CORRELATION BETWEEN THE ORIGINAL AND PREDICTED HUMAN PANEL DATA

Independent Variables	Intensity	Irritation	Pleasantness	Method
Lonestar (PC 1, 2, 3)	0.563	0.511	0.570	PCR
Lonestar (PC 1, 2)	0.634	0.583	0.663	PCR
Lonestar (PC 1)	0.605	0.525	0.639	PCR
Lonestar	0.651	0.609	0.671	PLS
Lonestar (PC 1, 2) & ppbRAE (Peak)	0.684	0.620	0.755	PCR
Lonestar & ppbRAE (Peak)	**0.720**	**0.667**	**0.842**	**PLS**

TABLE IV. SUMMARY OF CORRELATION BETWEEN THE MACHINE OLFACTION SYSTEMS AND THE HUMAN PANEL MEASUREMENTS

Machines	Human Panel Measurements		
	Intensity	*Irritation*	*Pleasantness*
ppbRAE	0.709	0.665	0.752
Lonestar	0.651	0.609	0.671
Combination	0.720	0.667	0.842

IV. CONCLUSIONS

The proposed machine olfaction system (MOS) can generate odor sensory information for air inside automobile cabins. The measurements of the Lonestar and ppbRAE alone have a correlation with human panel's measurements in the range of 0.609 to 0.752. A regression model based on the combination of the two instruments generates a prediction that increases the correlation with human panel tests (0.667 to 0.842) as shown in Table 4. Leaving out the samples of one of the vehicles validates the accuracy of the regression model. The results support the feasibility of replacing the human panel and suggest that including additional sensors in the system may further improve system performance.

REFERENCES

[1] T. Yoshida, I. Matsunaga, K. Tomioka, and S. Kumagai, "Interior air pollution in automotive cabins by volatile organic compounds diffusing from interior materials: I. survey of 101 types of Japanese domestically produced cars for private use," Indoor and Built Environment, vol. 15, pp. 425-444, 2006.

[2] M. Verriele, H. Plaisance, V. Vandenbilcke, N. Locoge, J. N. Jaubert, and G. Meunier, "Odor Evaluation and Discrimination of Car Cabin and its Components: Application of the "Field of Odors" Approach," Journal of Sensory Studies, vol. 27, pp. 102-110, 2012.

[3] A. M. MuÑOz and G. V. Civille, "Universal, product and attribute specific scaling and the development of common lexicons in descriptive analysis," Journal of Sensory Studies, vol. 13, pp. 57-75, 1998.

[4] P. Saha, S. Ghorai, B. Tudu, R. Bandyopadhyay, and N. Bhattacharyya, "Multi-class support vector machine for quality estimation of black tea using electronic nose," in Sensing Technology (ICST), 2012 Sixth International Conference on, 2012, pp. 571-576.

[5] P. Saha, S. Ghorai, B. Tudu, R. Bandyopadhyay, and N. Bhattacharyya, "Optimization of sensor array in electronic nose by combinational feature selection method," in Sensing Technology (ICST), 2012 Sixth International Conference on, 2012, pp. 341-346.

[6] A. Perera, A. Gomez-Baena, T. Sundic, T. Pardo, and S. Marco, "Machine olfaction: pattern recognition for the identification of aromas," in Pattern Recognition, 2002. Proceedings. 16th International Conference on, 2002, pp. 410-413 vol.2.

[7] J. W. Gardner and P. N. Bartlett, "A brief history of electronic noses," Sensors and Actuators B: Chemical, vol. 18, pp. 210-211, 1994.

[8] L. Dehan, F. Danjun, Y. Hao, and L. Zhimin, "A new processing technique for the identification of chinese herbal medicine," in Computational and Information Sciences (ICCIS), 2013 Fifth International Conference on, 2013, pp. 474-477.

[9] D. Luo and Y. Shao, "Discrimination of chinese herbal medicine by machine olfaction," Journal of Elect. Eng., vol. 11, pp. 630-636, 2013.

[10] T. Seesaard, T. Kerdcharoen, S. Kladsomboon, P. Lorwongtragool, and T. Kitiyakara, "Health status monitoring by discrimination of exhaled breath with an electronic nose," in Biomedical Engineering International Conference (BMEiCON), 2012, pp. 1-5.

[11] J. Feng, F. Tian, J. Yan, Q. He, Y. Shen, and L. Pan, "A background elimination method based on wavelet transform in wound infection detection by electronic nose," Sensors and Actuators B: Chemical, vol. 157, pp. 395-400, 2011.

[12] T. Pearce, S. Schiffman, H. Nagle, and J. Gardner, Handbook of machine olfaction: electronic nose tech.: John Wiley & Sons, 2006.

[13] L. Sirovich, "Turbulence and the dynamics of coherent structures. I-Coherent structures. II-Symmetries and transformations. III-Dynamics and scaling," Quarterly of applied math., vol. 45, pp. 561-571, 1987.

[14] R. Gutierrez-Osuna, lecture notes available: http://research.cs.tamu.edu/prism/lectures/pr/pr_l26.pdf

[15] R. Gutierrez-Osuna, "Pattern analysis for machine olfaction: a review," Sensors Journal, IEEE, vol. 2, pp. 189-202, 2002.

[16] P. Geladi and B. R. Kowalski, "Partial least-squares regression: a tutorial," Analytica chimica acta, vol. 185, pp. 1-17, 1986.